High gain isotropic rectenna

Erika Vandelle, Phi Long Doan, Do Hanh Ngan Bui, T.-P. Vuong, Gustavo Ardila, Ke Wu, Simon Hemour

High Gain Isotropic Rectenna

E. Vandelle[1], P. L. Doan[1], D.H.N. Bui[1], T.P. Vuong[1], G. Ardila[1], K. Wu[2], S. Hemour[3]

[1] *Université Grenoble Alpes, CNRS, Grenoble INP*, IMEP–LAHC, Grenoble, France*
[2] *Polytechnique Montréal, Poly-Grames, Montreal, Quebec, Canada*
[3] *Université de Bordeaux, IMS Bordeaux, Bordeaux Aquitaine INP, Bordeaux, France*

*Institute of Engineering University of Grenoble Alpes

{vandeler, buido, vuongt, ardilarg}@minatec.inpg.fr
phi-long.doan@etu.univ-grenoble-alpes.fr

ke.wu@polymtl.ca

simon.hemour@u-bordeaux.fr

***Abstract*— This paper introduces an original strategy to step up the capacity of ambient RF energy harvesters. The low rectification efficiency that comes from weak input power is enhanced through high gain antenna arrays that push the circuit to operate in a more efficient state. The prototype uses beam forming networks to build up a wide coverage since ambient energy can come from any direction, or the orientation of the rectenna may be unknown. By extending the operating range of rectifiers to higher input powers, the system operates as a very efficient narrow beam rectenna or as a synthetic high gain isotropic rectenna. The rectification efficiency pattern of one multi-beam rectenna, functioning in the 2.4 GHz band, is plotted and compared to a dipole rectenna's pattern. For a low incident power density of 4.10^{-5} mW.cm^{-2}, the rectification efficiency is largely improved in any direction : from 2.6% with a dipole rectenna up to 14%.**

***Index Terms*—Beam forming network (BSN), miniaturized Butler matrix, multiple beam antenna array, rectifier, high gain isotropic rectenna, efficiency pattern, RF energy harvesting.**

The recent exponential growth of Radio Frequency (RF) related devices has transformed our urban areas into promising ambient RF energy sources for powering ultra-low power IoT related electronic devices. The collection of such ambient energy requires the use of a rectifying antenna (rectenna) that captures the RF power and converts it into DC power. Still, the actual ambient RF power densities at communication frequency bands remain low and the major challenge faced by rectifiers is that low input power means low conversion efficiency, typically no more than 11% efficiency at -30 dBm and 2% at -40 dBm have been reached with Schottky diodes [1].

In the meantime, since the effective antenna aperture is proportional to the gain, implementing antenna arrays [2] or high-gain compact antennas [3] extend the amount of incident power at the rectifier input and therefore the rectification efficiency. Unfortunately, the directive nature of such antennas does not comply with RF energy harvesting applications where the location of the source is rarely known. Other solutions have been proposed like staggered pattern charge collectors (SPCC) [4] where high gain NxN sub arrays are utilized for increasing the beamwidth or 3D structures with multiple inkjet-printed antennas covering different directions [5].

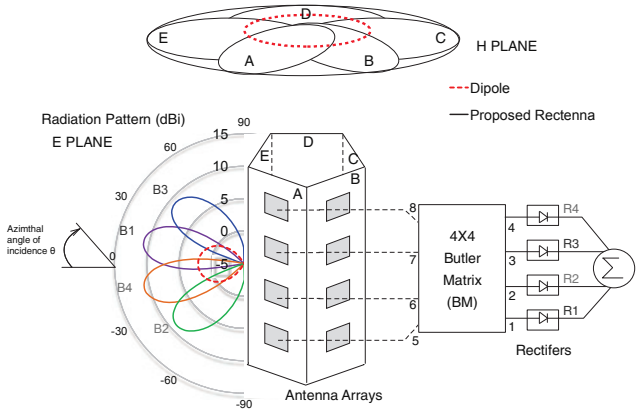

Fig. 1. Schema of the beam forming based RF energy harvester and its radiation pattern in the E plane and H plane of a linearly polarized radiation. The radiation pattern is compared to the radiation pattern of an omnidirectional dipole antenna.

In this paper, we propose the association of 5 antenna arrays, organized in a pentagon, with simple passive beam forming networks directly connected to rectifiers, as shown on figure 1. A passive beam forming network connected to a receiving antenna array can control the phases of incoming signals (at port 5, 6, 7 and 8) to redirect them into one input port (1, 2, 3 or 4) depending on the beam's orientation (B1, B2, B3 or B4). Therefore, associated to rectifiers (R1, R2, R3 and R4), the system allows the collection of RF energy with high gain antenna arrays without limitation of the beamwidth. With enhancement of the power at the rectifiers input, the rectification efficiency is increased in any direction. Positioned around a pole with the entire circuitry fitting inside, this multi beam rectenna could efficiently serve IoT applications. The benefits of the system are experimentally demonstrated here with an array of 4 rectangular patch antennas connected to 4 rectifiers via a 4x4 Butler Matrix for the collection of signals in the 2.4 GHz band. The rectification efficiency pattern [6] is measured for a low incident power density of 4.10^{-5} mW.cm^{-2} and compared with a dipole rectenna's pattern.

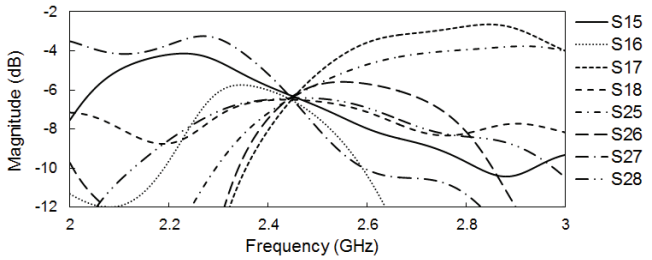

Fig. 2. Simulated amplitudes (dB) in transmission from ports 5,6,7 and 8 to ports 1 and 2.

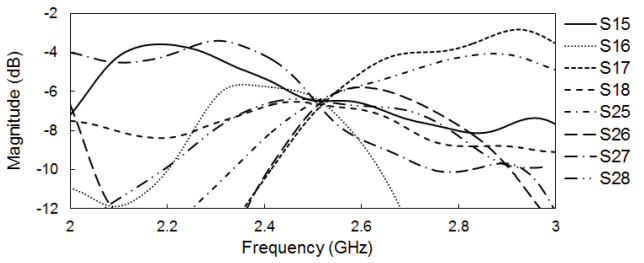

Fig. 3. Measured amplitudes (dB) in transmission from ports 5,6,7 and 8 to ports 1 and 2.

I. Components Design & Measurement

A. Butler Matrix

A standard 4x4 Butler Matrix (BM) is used to guide the RF signals captured by the antenna array into the rectifiers. This well-known passive and reciprocal beam forming network consists of 8 ports (see fig. 1), matched to 50 Ω, and is composed of 4 quadrature hybrid couplers, 2 crossovers and 2 phase shifters of 45°. The Butler matrix, visible on figure 10 (b), is designed with Momentum of Keysight ADS and fabricated on the ROGERS 4003 substrate with thickness 0.83 mm and relative permittivity 3.55.

Figure 2 and 3 plot the simulated and measured power distribution from ports 5, 6, 7 and 8 to ports 1 and 2 respectively. Note that the frequency response is shifted from 2.45 GHz in simulation to 2.52 GHz in measurement because of mechanical engraving. Otherwise the measurement of the power distribution is similar to simulation. Transmission coefficients from -6.3 dB to -6.9 dB indicate that ports 1 and 2 receive identical power from ports 5, 6, 7 and 8 at 2.52 GHz with 0.6 dB insertion loss on average. Figure 4 and 5 show the reflection at ports 1 and 2 and their isolation. Ports 1 and 2 are well matched and isolated at 2.52 GHz with transmission coefficients lower than -10 dB over a 25 % relative bandwidth.

Finally, table I presents the phase shifts at 2.52 GHz between ports 5, 6, 7 and 8 responsible for the concentration of the signals into port 1 or 2. Good agreement is found between ideal, simulated and experimental values with a maximum error in the measured phase shift as low as 3.4°. Due to the symmetry of the matrix, similar results are found for ports 3 and 4.

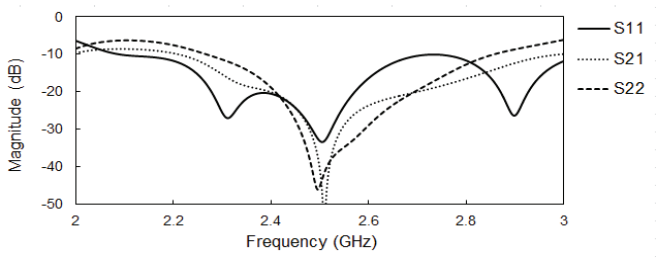

Fig. 4. Simulated reflection and isolation (dB) of ports 1 and 2.

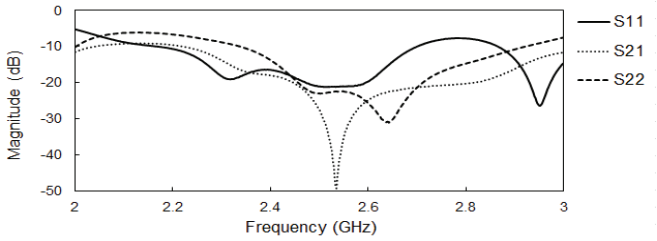

Fig. 5. Measured reflection and isolation (dB) of ports 1 and 2.

TABLE I
PHASE SHIFTS AT THE OUTPUT PORTS OF THE BUTLER MATRIX AT THE FREQUENCY OF OPERATION

Phase	Ideal	Simulated @ 2.45 GHz	Measured @ 2.52GHz
S(5,1) – S(6,1)	45°	43.311°	45.398°
S(6,1) – S(7,1)	45°	48.082°	48.455°
S(7,1) – S(8,1)	45°	42.373°	42.403°
S(5,2) – S(6,2)	-135°	-133.907°	-137.433°
S(6,2) – S(7,2)	-135°	-138.41°	-132.214°
S(7,2) – S(8,2)	-135°	-134.882°	-134.487°

As the lengths of the couplers lines are equivalent to $\lambda_o/4$, the dimensions of this matrix are expectedly large (112x130mm²) and need to be reduced for practical use. For this, a technique of miniaturization is experimented and consists of designing the couplers and crossovers of the BM with lumped elements [6]. The area of a coupler is reduced by a factor 4 with this approach compared to the classical design, leading to a high degree of miniaturization of the BM. However, the need for standard and available components reduces the range of optimization and results in more insertion losses.

Figure 6 and 7 (a) show the layouts of the classical BM and the BM obtained with lumped elements respectively, both designed on the RO4003 laminate with Momentum of Keysight ADS. A coupler with lumped elements, shown on figure 7 (b), is fabricated and experimental results appear to be well matched to simulation. Table II compares the performance in simulation of the two matrices: the area is reduced by a factor 6.5 with the miniaturized Butler matrix but the insertion losses are almost 2 dB higher on average. Thus, a tradeoff between size reduction and insertion loss needs to be found.

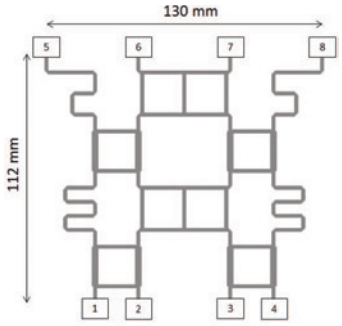

Fig. 6. Layout of the classical BM in microstrip technology on the laminate RO4003 h = 0.83 mm. f = 2.45GHz.

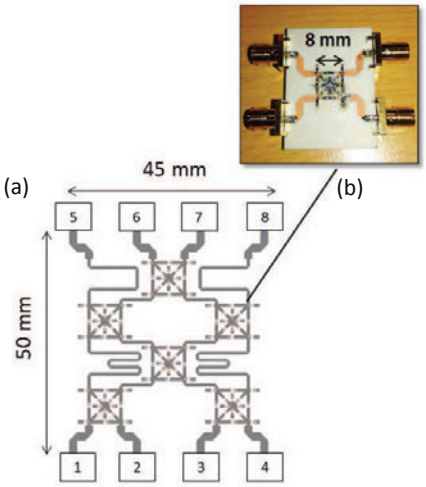

Fig. 7. (a) Layout of the miniaturized BM with lumped elements on the laminate RO4003 h = 0.83 mm. f = 2.45GHz. (b) Picture of a fabricated hybrid coupler.

TABLE II
COMPARISON OF THE SIMULATED PERFORMANCE OF THE TWO BUTLER MATRICES AT THE FREQUENCY OF OPERATION

Butler matrix	Relative bandwidth (-10 dB/ isolation, reflection)	Typical output @ 2.45 GHz (dB)	Phase error @ 2.45 GHz (°)	Area (mm²)
Classical	30 %	-6.6 ± 0.3	± 3.4	112x130
Miniaturized	10 %	-8.4 ± 0.7	± 3	50x45

B. Multiple Beam Antenna Array

Four rectangular patch antennas, matched to 50 Ω, are connected to the Butler matrix at ports 5, 6, 7 and 8 (see fig. 10 (b)) for the capture of vertically polarized RF signals. The antennas share the same ground and are spaced apart from each other by $\lambda_o/2$ to avoid coupling effects and limit grating lobes. The antenna array is simulated within the pentagon structure in CST Microwave Studio and fabricated on the RO4003 substrate with thickness 0.83 mm and relative permittivity 3.55.

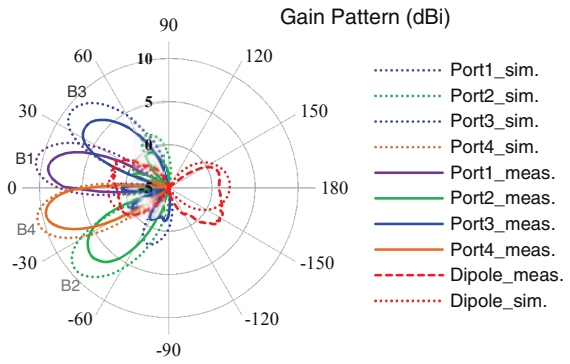

Fig. 8. Simulated and measured gain pattern (dBi) in the E plane, as a function of the azimuthal angle θ, of the multiple beam antenna array and of a vertically polarized dipole. f = 2.52 GHz.

As depicted in figure 8, the gain patterns of the multiple beam antenna array and of a half-wave dipole are measured in an anechoic chamber (in the E plane) at 2.52 GHz. As a proof of concept, this work uses the classical Butler matrix with output ports spaced apart from each other by $\lambda_o/2$. The radiation pattern resulting from the association of the antenna array to the Butler matrix widely covers the plane perpendicular to the array with 4 high gain beams that peak at 7 dBi for the side beams and up to 9.6 dBi for the center beams, while the dipole has a maximum gain of 2 dBi. The gain is improved of 5 to 7.6 dB over an angle of 120° in the E plane leading to at least 3 and to 6 times more power captured with this multiple beam antenna array than with a simple dipole. Note that side beams are inevitably less directive than center beams due to the geometry of the system.

C. Rectifier

The same rectifier is connected to ports 1, 2, 3 and 4 of the Butler matrix for the RF-DC rectification. It consists of a single series diode, a dc-pass filter and a resistive load. The single serial diode configuration is preferred when low input levels are considered. The rectifying element is the Schottky diode SMS7630, and the load is chosen to be a 5.1 kΩ resistor, close to the junction resistance of the diode (5 kΩ) [1]. A shunt capacitor of 2.2 nF acts like a DC pass filter and an open circuit stub between the diode and this filter helps in rectifying maximum current points. A Momentum co-simulation is performed in Keysight ADS with the Large Signal S-Parameters (LSSP) simulator for the evaluation of the input impedance. A L matching network is designed with a short circuit stub for an input power of -30 dBm. The rectifier is fabricated on the RO6002 substrate with thickness 1.524 mm and relative permittivity 2.94.

As presented on figure 9, the rectifier is matched to 50 Ω at 2.52 GHz for low input power from -40 to -25 dBm. Over this power range, the measured reflection coefficient S11 varies from -16.6 dB to -13.8 dB while the rectification efficiency ranges from 1.2 to 13.8%.

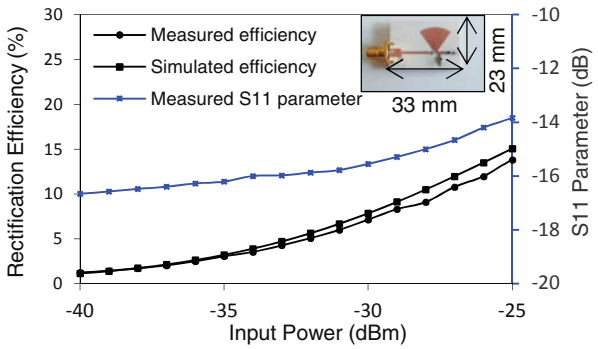

Fig. 9. Simulated and measured conversion efficiency (%) and S11 parameter of the rectifier (inside graph) as a function of the input power (dBm). f = 2.52 GHz.

II. Multi Beam Rectenna Measurement

The DC voltage is measured at a dipole rectenna's output and at the 4 rectifiers' outputs R1, R2, R3 and R4, connected to the multi beam antenna array. Measurement is performed in an anechoic chamber at frequency 2.52 GHz for a low omnidirectional incident power density level equivalent to 4.10^{-5} $mW.cm^{-2}$ at the system input.

Figure 10 (a) shows the rectification efficiency pattern simulated and measured for each rectifier in the elevation plane of the antennas. A picture of the multi beam rectenna is presented on figure 10 (b). Similar pattern as for the gain pattern is observed: 4 narrow beams are converted with high efficiency with the different rectifiers. The maximum efficiency is improved from 2.6% with the dipole rectenna to 11% with R2 and R3, 13% with R4 and up to 14% with R1. From figure 9, the maximum power received by the rectifier is estimated to progress from approximately -36 dBm with the dipole antenna to -27 or -24 dBm with the multi beam antenna array. Thus, while a simple dipole rectenna deliver a 5 nW power at maximum, the proposed multi beam rectenna is able to produce from 200 to 519 nW, depending on the orientation of the receiving beam, that is 40 to 100 times more DC power.

III. Conclusion & Perspectives

This paper demonstrates the benefits of a rectenna based on a beam forming network for the collection of very low RF power in the 2.4 GHz band. It is shown that the high gain and wide coverage of an antenna array coupled with a Butler matrix allows the rectification efficiency to be increased for any location of the RF energy transmitter compared to an omnidirectional dipole rectenna. The system can operate as a very efficient narrow beam rectenna: for a low incident power density of 4.10^{-5} $mW.cm^{-2}$, the rectification efficiency for 4 main beams is improved from 2.6 % with an omnidirectional dipole rectenna to 11, 13 and 14 % depending on the beam orientation. By interconnecting the rectifiers, each array can collect vertically polarized signals with high gain within a 120° angle in its perpendicular plane allowing the system to operate as a synthetic high gain isotropic rectenna.

In future work, further effort will be furnished to reduce the dimensions of the Butler matrices while trying to limit the insertion losses. The whole prototype will be implemented and techniques to obtain maximum gain patterns and for interconnecting the rectifiers will be investigated.

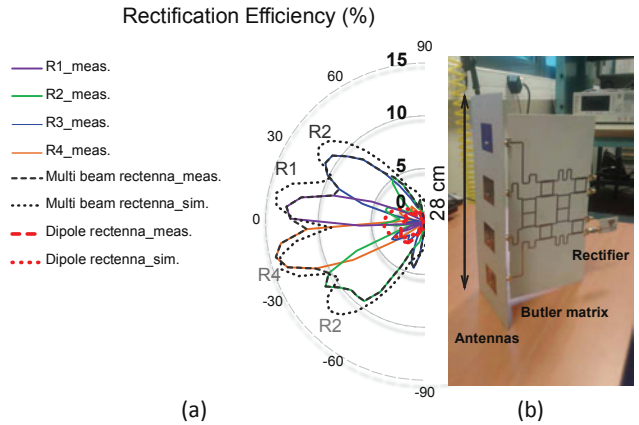

Fig. 10. Simulated and measured rectification efficiency pattern (%) in the E plane, as a function of the azimuthal angle θ, of rectifiers R1, R2, R3 and R4 of the proposed multi beam rectenna and of a dipole rectenna. f=2.52GHz. (b) Picture of the multibeam rectenna.

Ackowledgment

The authors would like to thank Nicolas Corrao and Antoine Pisa for their technical support for the fabrication of the circuits.

References

[1] C. H. P. Lorenz, S. Hemour and K. Wu, "Physical Mechanism and Theoretical Foundation of Ambient RF Power Harvesting Using Zero-Bias Diodes," in IEEE Transactions on Microwave Theory and Techniques, vol. 64, no. 7, pp. 2146-2158, July 2016.

[2] U. Olgun, C. C. Chen and J. L. Volakis, "Investigation of Rectenna Array Configurations for Enhanced RF Power Harvesting," in IEEE Antennas and Wireless Propagation Letters, vol. 10, no. , pp. 262-265, 2011.

[3] H. Sun, Y. x. Guo, M. He and Z. Zhong, "Design of a High-Efficiency 2.45-GHz Rectenna for Low-Input-Power Energy Harvesting," in *IEEE Antennas and Wireless Propagation Letters*, vol. 11, no. , pp. 929-932, 2012.

[4] J. Kimionis, M. Isakov, B. S. Koh, A. Georgiadis and M. M. Tentzeris, "3D-Printed Origami Packaging With Inkjet-Printed Antennas for RF Harvesting Sensors," in *IEEE Transactions on Microwave Theory and Techniques*, vol. 63, no. 12, pp. 4521-4532, Dec. 2015.

[5] B. R. Marshall, C. R. Valenta and G. D. Durgin, "DC power pattern analysis of N-by-N staggered pattern charge collector and N2 rectenna array," 2013 IEEE Wireless Power Transfer (WPT), Perugia, 2013, pp. 115-118.

[6] Z. Popović, E. A. Falkenstein, D. Costinett and R. Zane, "Low-Power Far-Field Wireless Powering for Wireless Sensors," in *Proceedings of the IEEE*, vol. 101, no. 6, pp. 1397-1409, June 2013.

[7] E. Gandini, M. Ettorre, R. Sauleau and A. Grbic, "A Lumped-Element Unit Cell for Beam-Forming Networks and Its Application to a Miniaturized Butler Matrix," in *IEEE Transactions on Microwave Theory and Techniques*, vol. 61, no. 4, pp. 1477-1487, April 2013.